International Journal of Applied Engineering Research ISSN 0973-4562 Volume 10, Number 14 (2015) pp 34339-34345
© Research India Publications. http://www.ripublication.com

Design of a Novel RF MEMS Dual and Quad Output Switches For Satellite Payload Applications

[1]John Wiselin, [2] B.S. Sreeja, [3]K.Sureshkumar, [2] C.Joshitha [2]V.I. Nandhini, [2]Roshini Shetty, [2]K. Suneri and [2]S. Yazhini
[1]Department of EEE, Travancore College of Engineering, Kerala India
[2]Department of ECE, SSN College of Engineering, Chennai,India
[3]IFET College of engineering, Vilupuram, India
sreejaabs@gmail.com

Abstract- This paper presents the design and performance analysis of a cantilever based microelectromechanical systems (MEMS) switch cell which could be used for switch matrices for performance in the Ku band of frequency. Two designs have been developed that use electrostatic actuation mechanism to facilitate operations in which one input is available to more than one output. Variation in the cantilever beam design to reduce the spring constant has been used to design a dual output and a quad output switch. The designed structure is simulated and characterized using Intellisuite and HFSS software tools. An insertion loss of around 0.8dB and isolation of 47dB for the dual output structure and insertion loss of around 2.2dB and isolation in the range of 57dB for the quad output structure has been observed in the Ku band of frequency(12-18 GHz).

Keywords- RF switch matrix, MEMS, Satellite payload, IntelliSuite, Simulation, High Frequency Structure Simulator(HFSS)

1. Introduction

Micro-electro-mechanical systems (MEMS) is a mixture of mechanical and electrical structures that are typically sized down to the micrometer range. The main research areas of MEMS include RF MEMS Switches, RF MEMS passives, Micro-machined transmission lines, Micro-machined Antennas, MEMS resonators, MEMS mirrors and FBAR (Film Bulk Acoustic Resonators) devices[Rebeiz 2003]. Among these devices RF MEMS switch is the most extensively analyzed component. Enhanced performance parameters can be achieved from conventionally used mechanical and waveguide switches. But these switches are bulky and consume high power when they are used in large numbers as switch matrix. Moreover these switches very low switching speed. The shortcomings of mechanical switch can be trounced by the use of semiconductor switches; however these switches have poor RF performance. Better tradeoff between these two switches can be obtained by using RF MEMS switches. Despite-of its packaging issues and reliability[Goldsmith and at al 2007], major benefits of RF MEMS switches are good RF performance, light weight, high speed and very low power consumption[Peroulisand et al, 2004].

The basics of MEMS, different types of switch configurations, the actuation mechanisms and fabrications of the switches were studied in [Varadhan and et al, 2003]. Pros and cons of various actuation mechanisms were also discussed. Electrostatic actuation was suggested to be the best out of the four mechanisms. [Rebeiz 2003] introduced the two basic configurations of RF MEMS switches namely series contact and shunt capacitive switches. Further, the variation of actuation voltage with the spring constant of the cantilever beam, mechanical modeling and factors affecting reliability of the switch were also discussed.

Novel multi-port RF MEMS switches such as SP3T, C-type and R-type switches and thermally actuated multi-port switches that include SPST, SP2T and C-type configurations have been proposed and investigated in [Daneshmand 2006, Farina and et al 2004, Grenier and et al 2005;McErlean and et al 2005;Muldavin and et al 2001, Uno and et al 2009]. This thesis has introduced a novel concept for 3D RF MEMS switches based on integrating MEMS actuators with waveguide structures. Prototype units for both ridge and coaxial MEMS based SPST and C-type switches have been fabricated and tested. The measured results verify the concept demonstrating a good return loss of -20dB and a high isolation of 35-40dB over band of interest. Overall, the focus of this thesis has been on multi-port switches and switch matrices for redundancy and signal routing in satellite communication.

In [Jaafar and et al, 2006] high performance RF MEMS switch with low voltage actuation, high isolation and low insertion loss was designed and simulated using IntelliSuite. The essential parameters of the RF MEMS switches obtained in this paper have proved that they are suitable for microwave application as all the parameters simulated are excellent. Besides that, few things could be concluded while optimizing the RF MEMS switch designs such as the height of air gap has negligible effect on the maximum displacement in each direction; larger value of the height of air gap will increase the actuation voltage consumed by the switch and design of support beam with lower spring constant will consume less actuation voltage during operation.

The novel configurations of planar multiport radio-frequency (RF) micro-electromechanical systems (MEMS) C-type and R-type switches and redundancy switch matrices for satellite communications were investigated in [Daneshmand and et al, 2007]. The proposed C-type switch exhibits an insertion loss of less than 0.3 dB and isolation of about 25 dB at satellite C-band frequency range. The novel R-type switch showed an insertion loss of better than 0.4 dB and an isolation of better than 25 dB at C-band. This was the first time that an R-type RF MEMS switch is ever reported. Several of these switches are integrated in the form of redundancy switch matrices, and two novel monolithic five to seven redundancy switch matrices were developed, fabricated, and tested. It was also shown that the additional operating state of the R-type switch not only decreased the number of elements by 50% but also reduced the size drastically.

The novel approach to implement RF MEMS large size switch matrices was studied in [Chan and et al, 2008]. The concept was based on the implementation of a crossbar switch matrix and the introduction of unique switch cells that can be easily used to expand the matrix size.

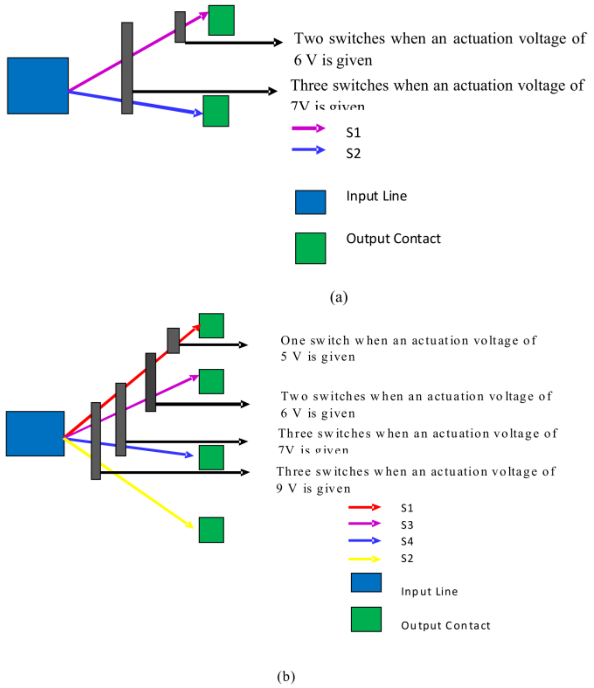

Fig 1. Proposed topology of the switch structure (a) Dual output structure (b) Quad output structure

Novel series contact cantilever beams were used to implement the entire structure. The measured results for the entire switch cell showed excellent insertion loss of 0.5dB, return loss of better than -20dB and isolation of -25dB for the thru path. The turn state of the switch showed a good performance of 0.4dB insertion loss, -18dB return loss and better than -25dB isolation for the frequency band of interest. A 3×3 switch matrix was implemented that showed 98% size reduction in comparison with the previously reported RF MEMS switch matrices.

Due to the high speed and less weight especially when using as switch matrices RF MEMS switches are of special interest for satellite payload applications. Even though RF MEMS switches are rigorously investigated by various researchers, these switches are not yet implemented in satellite payload due to its isolation and insertion loss requirements. Further satellite payload will require signal rerouting such that a single input is available at more than one output ports. One such topology has been proposed in this article and the proposed structure is shown in Fig 1.

There are several mechanisms for actuating a RF switch. These include electrostatic, electromagnetic, thermal switching. Of these, electrostatic switching is found to be the most advantageous because of its low power consumption and ease of implementation. Series contact switches and shunt capacitive switches are the two categories of RF switches that use electrostatic switching. One of the key aspects of the performance of a switch that uses electrostatic switching is its actuation voltage, which is defined as the voltage applied between the top and bottom electrode so as to enable them to come into contact with each other. This key factor can be lowered by modeling the design of the switch like that of a cantilever.

The RF performance of a switch is determined by its insertion loss and isolation at the desired range of frequencies [Liu 200;, Sahaand et al 2005; Goldsmith and et al 1998]. Insertion loss is the loss of signal power caused by introducing the switch in the transmission line. Isolation of a switch is the extent to which unwanted signal at a port is attenuated. For implementation of the switch in a satellite payload, insertion loss of less than 2.5dB and isolation greater than 20dB is desired up to a frequency of 15GHz.

The cantilever switch shown in Fig.2 consists of a top and bottom electrode separated by an air gap. When an actuation voltage is applied between these two electrodes, the electrostatic force generated will pull the cantilever beam down thus closing the gap in the transmission line and completing the conducting path.

Fig.2. Cross section of typical MEMS cantilever switch [Liu 2007]

2. Proposed switch design

A basic cantilever switch consists of a silicon substrate on top of which lies the bottom electrode. An air gap separates the top and bottom electrode as shown in Fig 3.The material used for the top and bottom electrodes may be a good conducting material like aluminium or gold. On simulation of this basic cantilever structure, it was observed that the actuation voltage was in the range of 30V which is quite high.From (3), it has been observed that the actuation voltage is directly proportional to the spring constant of the beam which can be varied by changing the dimensions and structure of the beam as well as the materials used. The spring constant of the beam is also determined by the Young's modulus and Poisson ratio of the beam and its residual stress. It can be expressed as

$$k = 32Ew\left(\frac{t}{l}\right)^{3}\left(\frac{27}{49}\right) + 8\sigma(1-v)w\left(\frac{t}{l}\right) \quad (1)$$

where E is the Young's modulus which accounts for the dependence of spring constant on the material used. The dimensions of the beam, i.e. width w, thickness t and length l also determine the spring constant as shown in(1). The second term in the above expression takes into account the biaxial residual stress, σ which is induced during the fabrication process, and Poisson's ratio *v*. This expression is valid for a beam with both the ends fixed. However for the case of a beam with one end fixed the second term becomes zero thus modifying the expression to

$$k = \left(\frac{2}{3}\right) E w \left(\frac{t}{l}\right)^3 \quad (2)$$

Further the actuation voltage of the beam, i.e., the voltage at which the cantilever beam moves down and makes contact between the top and bottom electrodes is a function of the spring constant and is expressed as

$$V = \sqrt{\frac{8k}{27\varepsilon_0 W w} d^3} \quad (3)$$

where d is the height of the air gap that separates the two electrodes, W is the width of pull down electrode, ε_0 is the permittivity of free space, w is the width of the beam and k is the spring constant.

Taking into consideration all the factors discussed above, it is evident that by modifying the spring constant by varying the beam design and materials used the actuation voltage of the switch can be varied to a considerable extent. This has been made use of to design a novel switchthat can enable single input to multiple output operation which is essential in a satellite payload. The basic structure proposed is shown in Fig 3.

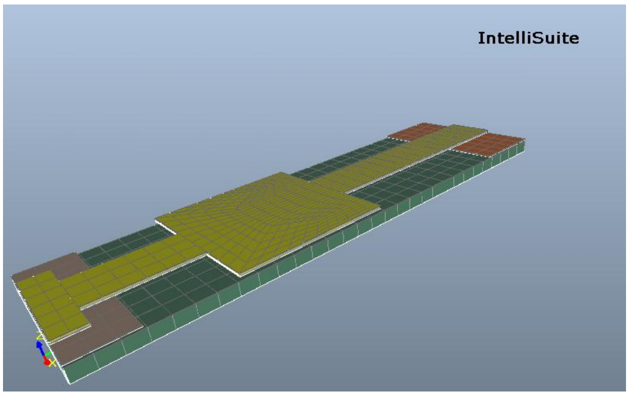

Fig 3. Proposed structure of the RF switch

Table 1: Comparison of theoretical and simulated values of actuation voltage for different air gaps

Airgap (µm)	Theoretical calculation of actuation voltage (v)	Simulated of actuation voltage (v)
0.8	6.77	5.0
1	9.46	7.0
1.4	12.675	9.0

Arrange of voltage from 2V to 14V was applied to the above structure and it was observed that for an air gap of 0.8µm the actuation voltage was found to be 5V which can be seen from the Fig.4. This is much lesser than the value obtained for the basic cantilever structure which was 35V. The height of the air gap was further varied and the theoretical and simulated values of the actuation voltage were calculated. The actuation voltage was calculated using the formula in equation 3. Since the air gap is directly proportional to the actuation voltage, it was observed that the actuation voltage increases with increase in the height of the air gap as shown in Table.1.

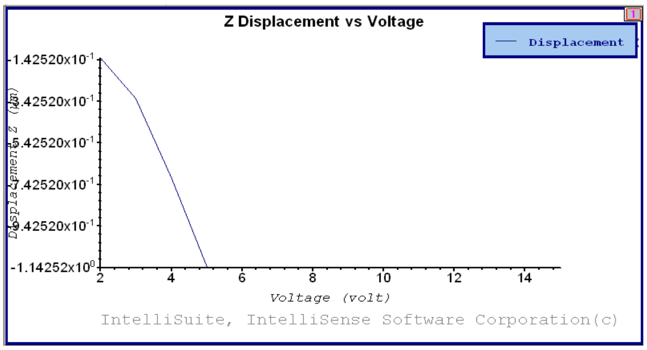

Fig 4: Variation of Z-displacement with the actuation voltage

The structure in Fig.5 represents a single input to dual output switch. The dimension of the beam and the material used for each electrode has been varied such that each switch operates at a different actuation voltage. The blue color strip represents the common RF line input. The design of each layer is shown in Fig.4. Intelli Suite was used to build the 3D structure and perform Thermo Electro Mechanical analysis to study the variation of displacement with applied voltage [Haixia 2001].

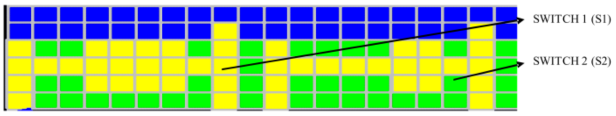

Fig.5. Single input dual output switch structure

The same logic was extended to design a single input to four output switch. In order to introduce variation in the actuation voltage the beam design for each switch is different and hence the spring constant for each switch is different

[Pacheco and et al 2000; Kiang and et al 2000; Chu and et al 2007]. The structure of the quad switch is as shown in Fig.6. The blue strip at the centre is the common RF input line.

Dimensions of the dual output structure:

- Total length = 200 µm
- Total width = 60 µm
- Length of the switch = 90 µm
- Width of the switch = 50 µm
- Width of the RF line = 20 µm
- Height of air gap = 1.8 µm

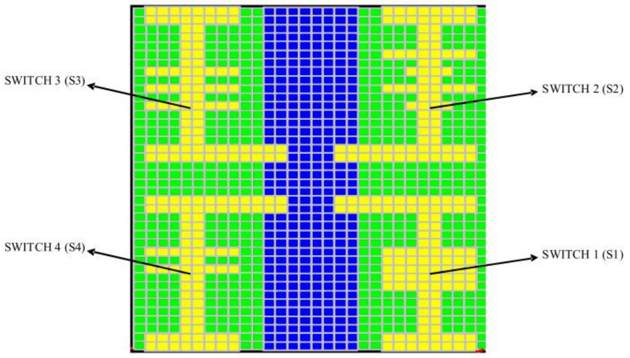

Fig.6. Structure of quad switch

Dimensions of the quad output structure:

- Total length = 400 µm
- Total width = 300 µm
- Length of the switch = 180 µm
- Width of the switch = 120 µm
- Width of the RF line = 80 µm
- Height of air gap = 0.5 µm

The structure is composed of several layers. The layer arrangements of both the structures are shown in Fig 6 and Fig 7. Layer 0 is the silicon substrate on top of which rests the cantilever structure. Layer 1 shown in green represents silicon nitride on top of which lies the electrodes and the common RF line which is composed of a good conducting material, aluminium, represented in blue [Sharma and et al 2012]. Layer 4 and Layer 5 form the cantilever beam whose shape and dimension is altered for every switch. The rest of the structure remains same except for the variation in air gap and material used for the electrode.

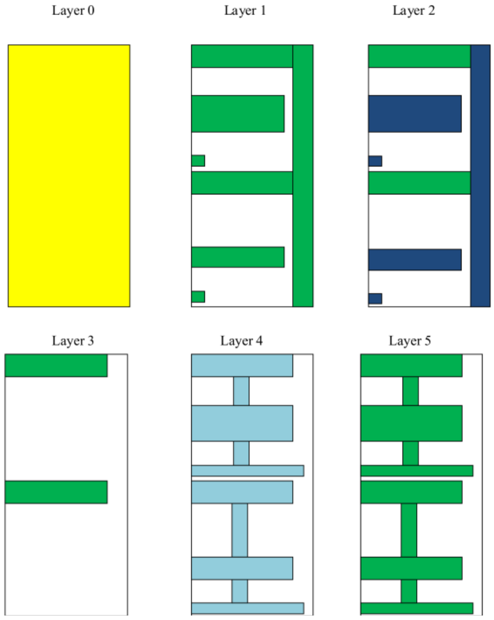

Fig.7. Design of the single input dual output structure

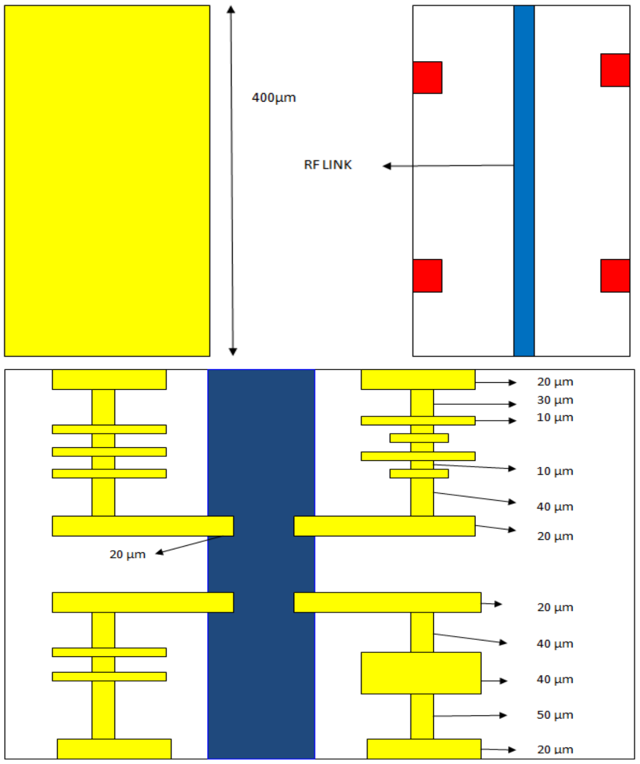

Fig:8 Design of single input quad output structure

3. Results and discussions:

A. Analysis on Actuation voltage

The designed structures were simulated using Thermo Electro Mechanical module in Intelli Suite. The variation of displacement with applied voltage was studied to determine the actuation voltage of each switch. For the structure in Fig.2,an air gap of 1.8µm resulted in an actuation voltage of 9.5V and 11V respectively for switch S1 and S2. At a voltage of less than 9.5V both the switches are in the OFF state. On increasing the voltage beyond 9.5V but less than 11V, S1 turns ON while S2 continues to remain in the OFF state. Further increasing the voltage beyond 11V turns both the switches to the ON state. This thus enables single input to dual output operation. The displacement of the switch at a voltage of 11V is depicted in Fig.9.

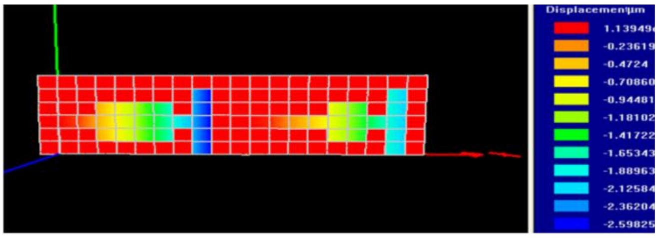

Fig.9. Z-displacement of the Dual output structure

The working range of the switch has been summarized in Table2. The values in bold signifies the switch in ON position.

Table 2: Summary of operation of dual output switch

Actuation Voltage (v)	S1(µm)	S2(µm)
9.5	**1.8***	1.47
11	**2.59***	**1.88***
* Represents ON position		

The above explanation holds good for the case of quad output switch. The actuation voltage for switches S1, S2, S3 and S4 in Fig.3 is 5V, 6V, 7V and 9V respectively for an air gap of 0.5µm. All the switches will be in the OFF state for a voltage less than 5V. At a voltage of 9V and above all the switches conduct as the top and bottom electrodes of all the switches come in contact with each other. The switching action of the individual switches can be controlled by applying an intermediate voltage between 5V and 9V. Fig.7 depicts the displacement of the switches at a voltage of 6V. It can be seen that switches S1 and S2 are in the ON state while S3 and S4 remain in the OFF state. The displacement of the single input quad output structure is shown in Fig 10. The displacement of the switch for various actuation voltages is summarized in Table 3.

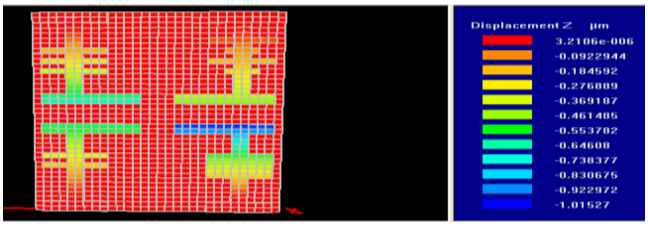

Fig.10. Z-Displacement of the quad output structure

Table 3: Summary of operation of quad output switch

Actuation Voltage (V)	S1(µm)	S2(µm)	S3(µm)	S4(µm)
5	**0.67***	0.18	0.42	0.36
6	**1.01***	0.27	**0.73***	0.43
7	**1.05***	0.28	**0.76***	**0.67***
9	**1.74***	**0.57***	**1.26***	**1.11***
* Represents ON position				

B. RF PERFORMANCE:

RF parameter is essential for the MEMS switch as it will apply in communication at high frequency. Thus, these microwave parameters should be considered when designing the switch. In on-state condition, the switch disconnects the input port to the output port while during the off-state condition; the switch is configured to connect the two ports.

Both insertion loss and isolation values can be obtained from the transmission coefficient, in decibels, between the input and output ports of transmission line. Smaller insertion loss represents loss between transmission efficiency while larger isolation represent very small coupling between input and output terminal when switch is in the up-state.

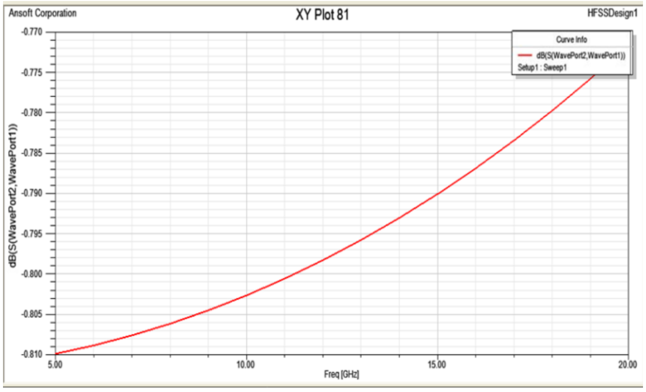

Fig.11. Insertion loss of the dual output structure

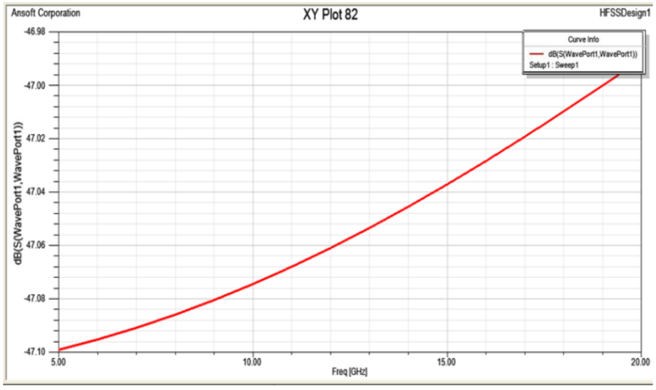

Fig.12. Isolation of the dual output structure

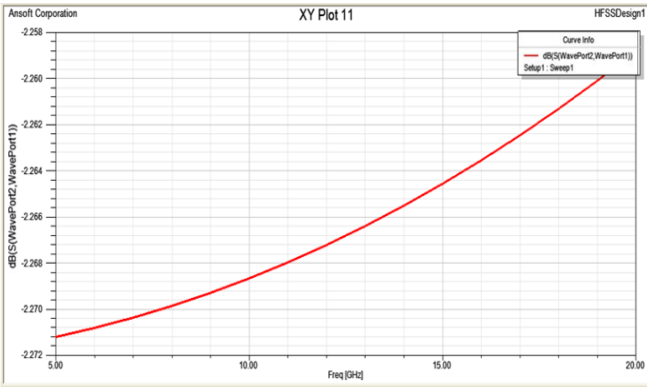

Fig.13. Insertion loss of the quad output structure

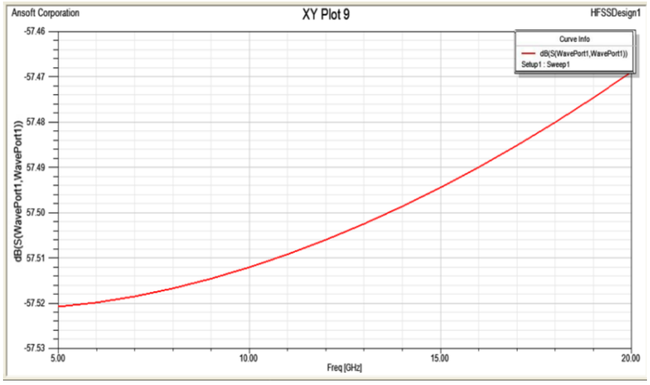

Fig.14. Isolation of the quad output structure

The RF performance of the switch was measured by simulating the structure using Ansoft's High Frequency Structure Simulator (HFSS) in the Ku band of frequency[Yamane and et al 2011]. The dual output switch had insertion loss in the range of 0.8dB while isolation of around 47dB was observed from Fig.11 and Fig.12 respectively. The simulation results of the quad output switch predicted insertion loss of about 2.2dB and isolation of around 57dB which can be seen from Fig. 13 and Fig.14 respectively.

The RF performance of the switch cell designed is compared with the existing switch cell types and is shown in Table 4. The simulated results show that both the switches offer comparatively better isolation characteristics in the Ku band of frequency. Hence these type of switch cells can be used in developing switch matrices for satellite payload applications.

Table 4 Performance comparison of different switch cell types with the proposed work

Switch Cell type	RF performance		Operating Frequency (G Hz)
	Insertion Loss (dB)	Isolation Loss (dB)	
C Type [Schaffner and et al 2003]	0.5	25	0–25
R Type [Daneshmand and et al 2006]	1	20	0–20
T Type [Chan and et al 2008]	1	30	0–20
Cross bar [Chan and et al 2008]	0.5	35	0–20
This work* Dual Output Quad Output	0.8 2.2	47 57	0-20 0-20
* Simulated Results			

Conclusion:

A novel cantilever beam MEMS switch has been designed and simulated that facilitates single input dual output and quad output operation. The dual output and quad output designs have demonstrated good RF performance in the Ku band of frequency. The dual output structure has exhibited insertion loss of less than 0.8dB and isolation of 47dB while the same values for the quad output structure are 2.2dB and 57dB. The actuation voltage of the individual switches in both the structures is less than 11V. The RF performance of the switch indicates that it is suitable for application in a satellite payload. Further it is expected to design switch matrices which could be used in satellite payload applications.

References

[1] Chu, C.H.; Shih, W.P.; Chung, S.Y.; Tsai, H.C.; Shing, T.K.; Chang, P.Z. A low actuation voltage electrostatic actuator for RF MEMS switch applications, Journal of Micromechanics and Microengineering, July 2007; pp. 1649-1656.15.

[2] Daneshmand, M.; Mansour, R.R. Redundancy RF MEMS Multiport Switches and Switch Matrices, Journal of Microelectromechanical Systems, Vol. 16, No. 2, April 2007; pp. 296-303.

[3] Daneshmand, M; Multi-port RF MEMS switches and switch matrices, Ph.D. dissertation, University of Waterloo, Waterloo, Canada, Jan 2006.

[4] Farina, M.; Farinelli, P.; Mezzanotte, P.; Sorrentino, R.; Blondy, P. A New Single-Pole Double-Throw MEMS Switch Topology, 34th European Microwave Conference, Amsterdam, 2004.

[5] Goldsmith C.L.; Yao, Z.; Eshelman, S.; Deiston, D. Peformance of Low-Loss RF MEMS Capacitive Switch, IEEE Microwave And Guided Wave Letters, 1998, pp. 269-271

[6] Goldsmith, C.; Maciel, J.; McKillop, J. Demonstrating Reliability, IEEE Microwave Magazine, December 2007.

[7] Grenier, K.; Dubuc, D.; Ducarouge, B.; Conedera, V.; Bourrier, D.; Ongareau, E.; Derderian, P.; Plana, R. High power handling RF MEMS design and technology in Proc. 18th IEEE Int. Conf. Micro Electro Mechanical Systems, Miami, FL, 2005; pp. 155–158.

[8] Haixia, Z.; Yilon, H.; Zhiyong, X.; Dongmei, L. Design of a Novel Bulk Micro-machined RF MEMS Switch, International Conference on Micro and Nano Systems. 2002.

[9] Jaafar, H.; Nan, F.L.; Yunus, N.A.M. Design and Simulation of High Performance RF MEMS Series Switch, RSM2011 Proc, 2011.

[10] Kiang, K.S.; Chong, H.M.H.; Hwang, C.J.; Lok, L.B.; Elgaid, K.; Kraft, M. Development of a low actuation voltage RF MEMS Switch,

[11] Liu, A.Q.; Yu, A.B.; Karim, M.F.; Tang, M. RF MEMS Switches and Integrated Switching Circuits, Journal of Semiconductor Technology and Science, Vol. 7, No. 3, September 2007; pp. 166-176.

[12] Liu, L. High Performance RF MEMS Series Contact Switch-Design and Simulations, Electronic Components and Technology Conference, 2007.

[13] McErlean, E. P.; Hong, J.S.; Tan, S. G.; Wang, L.; Cui, Z.; Greed, R. B.; Voyce, D. C. 2 X 2 RF MEMS switch matrix, IEEE Proc. Microwave Antennas Propagation, Vol. 152, No. 6, 2005; pp. 449–454.

[14] Muldavin, J.B.; Rebeiz, G.M. RF MEMS Switches and Switch Circuits, IEEE Microwave magazine. 2001; pp. 59-71

[15] Pacheco, S.P.; Katehi, L.P.B.; Nguyen, C.T.C. Design of Low Actuation Voltage RF MEMS Switch, IEEE. 2000.

[16] Peroulis, *D.; Pacheco, S.P.; Katehi, L.P.B.* RF MEMS Switches With Enhanced Power handling Capabilities, IEEE Transactions on Microwave Theory and Techniques, Vol. 52, No.1, January 2004.

[17] Rebeiz, G.M. *RF MEMS: Theory, Design, and Technology*; John Wiley & Sons: Hoboken, NJ, USA, 2003; pp. 239-256.

[18] Saha, S.C.; Singh, T.; Saether, T. Design and Simulation of RF MEMS Switches for high switching speed and moderate voltage operation, Research in Microelectronics and Electronics, 2005.

[19] Sharma, A. K.; Gupta, N. Material Selection of RF-MEMS switch used for Reconfigurable Antenna using Ashby's Methodology, Progress In Electro magnetics Research Letters, Vol. 31. 2012; pp. 147-157.

[20] Uno, Y.; Narise, K.; Masuda, T.; Inoue, K.; Adachi, Y.; Hosoya, K.; Seki, T.; Sato, F. Development of SPDT-Structured RF MEMS Switch, Transducers 2009, Denver, CO, USA, June 2009.

[21] Varadan, V.K.; Vinoy, K.J.; Jose, K.A. *RF MEMS and Their Applications*; New York: Wiley, 2003.

[22] Yamane, D; Sun, W; Seita, H, Kawasaki, S; Fujita, H; Toshiyoshi, H. A Ku-band Dual-SPDT RF-MEMS Switch by Double-Side SOI Bulk Micromachining, Journal of Micro electromechanical Systems, Vol. 20, No. 5, October 2011; pp. 1211-1221.

[23] Schaffner J. H., A. E. Schmitz, T. Y. Hsu, D. T. Chang, R. Y.Loo, and D. F. Sievenpiper, “Metal contact RF MEMS switchelements for ultra wideband RF front end systems,” in *Proc.2003 IEEE Conf. Ultra Wideband Systems and Technologies*, Nov.16–19, 2003, pp. 129–132.

[24] DaneshmandM. and R. R. Mansour, “C-type and R-type RFMEMS switches for redundancy switch matrix applications,”in *IEEE MTT-S Int. Microwave Symp. Dig.*, 2006, pp. 144–147.

[25] ChanK., M. Daneshmand, R. R. Mansour, and R. Ramer, “MonolithicMEMS T-type switch for redundancy switch matrix applications,”in *Proc. European Microwave Integrated Circuits Conf.*, Oct.2008, pp. 1513–1516.

[26] Chan K, M. Daneshmand, R. R. Mansour, and R. Ramer, “Monolithiccrossbar MEMS switch matrix,” in *IEEE MTT-S Int. MicrowaveSymp. Dig.*, Atlanta, GA, June 2008, pp. 129–132.